Journal of Invertebrate Pathology 203 (2024) 108065

Contents lists available at ScienceDirect

Journal of Invertebrate Pathology

journal homepage: www.elsevier.com/locate/jip

Quantification of *Photobacterium swingsii* and characterisation of disease progression in the New Zealand Greenshell™ mussel, *Perna canaliculus*

Awanis Azizan [a], Andrea C. Alfaro [a,*], Leonie Venter [a], Diana Jaramillo [b], Mark Bestbier [b], Peter Bennett [b], Jonathan Foxwell [b], Tim Young [a,c]

[a] *Aquaculture Biotechnology Research Group, Department of Environmental Sciences, School of Science, Auckland University of Technology, Private Bag 92006, Auckland 1142, New Zealand*
[b] *Animal Health Laboratory, Ministry for Primary Industries, PO Box 2526, Wellington 6140, New Zealand*
[c] *Centre for Biomedical & Chemical Sciences, School of Science, Auckland University of Technology, Auckland, New Zealand*

ARTICLE INFO

Keywords:
Greenshell™ mussels
Haemocytes
Perna canaliculus
Photobacterium
Pathogenesis
qPCR

ABSTRACT

Greenshell™ mussels (*Perna canaliculus*) are endemic to New Zealand and support the largest aquaculture industry in the country. *Photobacterium swingsii* was isolated and identified from moribund *P. canaliculus* mussels following a mass mortality event. In this study, a challenge experiment was used to characterise, detect, and quantify *P. swingsii* in adult *P. canaliculus* following pathogen exposure via injection into the adductor muscle. A positive control (heat-killed *P. swingsii* injection) was included to account for the effects of injection and inactive bacterial exposure. Survival of control and infected mussels remained 100% during 72-hour monitoring period. Haemolymph was sampled for bacterial colony counts and haemocyte flow cytometry analyses; histology sections were obtained and processed for histopathological assessments; and adductor muscle, gill, digestive gland were sampled for quantitative polymerase chain reaction (PCR) analyses, all conducted at 12, 24, 48 h post-challenge (hpc). The most profound effects of bacterial injection on mussels were seen at 48 hpc, where mussel mortality, haemocyte counts and haemolymph bacterial colony forming were the highest. The quantification of *P. swingsii* via qPCR showed highest levels of bacterial DNA at 12 hpc in the adductor muscle, gill, and digestive gland. Histopathological observations suggested a non-specific inflammatory response in all mussels associated with a general stress response. This study highlights the physiological effects of *P. swingsii* infection in *P. canaliculus* mussels and provides histopathological insight into the tissue injury caused by the action of injection into the adductor muscle. The multi-technique methods used in this study can be applied for use in early surveillance programs of bacterial infection on mussel farms.

1. Introduction

Perna canaliculus, Greenshell™ mussels are the most important aquaculture species in New Zealand, typically sold as a variety of food products worldwide (Miller et al., 2023, Ericson et al., 2022). Aquaculture development and increasing disease occurrences have prompted interest in studies on aquatic diseases which are likely to keep growing in the face of future threats from climate change, invasive species and pollution (Lane et al., 2022). Even though the *P. canaliculus* mussel industry has experienced relatively few disease issues, the presence of pathogens and parasites continue to be reported (Castinel et al., 2019). *Vibrio* spp. such as *Vibrio splendidus*, a *Vibrio coralliilyticus/neptunis*-like isolate (Kesarcodi-Watson et al., 2009), *Vibrio mediterranei* (Azizan et al., 2023) and *Photobacterium swingsii* (Azizan et al., 2022) have been associated with mortalities in *P. canaliculus*.

Photobacterium is one of the eight genera in the Family Vibrionaceae (order Vibrionales, class Gammaproteobacteria) and is the largest genus after *Vibrio* (Labella et al., 2017). Several species in this genus, including *P. rosenbergii, P. swingsii, P. jeanii, P. sanctipauli, and P. damselae,* have been shown to cause pathologies in animal hosts, as reviewed by Labella et al. (2017). Of particular interest for the current research are *P. swingsii* infections that have previously been detected in diseased Pacific oysters (*Crassostrea gigas*) (Gomez-Gil et al., 2011), wild spider crabs (*Maja brachydactyla*) (Gomez-Gil et al., 2011), blue mussels (Eggermont et al., 2017), abalone (Jiang et al., 2013) and octopus (Fichi et al., 2015). Additionally, mussels injected with *P. swingsii* showed high mortality at

* Corresponding author.
E-mail address: andrea.alfaro@aut.ac.nz (A.C. Alfaro).

https://doi.org/10.1016/j.jip.2024.108065
Received 12 May 2023; Received in revised form 17 January 2024; Accepted 18 January 2024
Available online 19 January 2024

48 h post-challenge, along with expression of virulence genes *hsp60*, *zm*, *vcpA*, *toxR*, *ompU*, *mshA*, *chi*, *lip*, and *plp*, suggesting pathogenesis of this bacterium to *P. canaliculus* (Azizan et al., 2022). Despite advances that have been made, the mechanisms of bacterial pathogenesis of *P. swingsii* in *P. canaliculus* mussels are poorly understood.

Monitoring programs use a variety of diagnostic techniques to assess the condition and health status of farmed and wild mussel populations (Webb and Duncan, 2019). The most used methods for disease testing include bacterial culture, PCR, enzyme-linked immunosorbent assays (ELISA), histopathology, fluorescent *in situ* hybridisation (FISH) and immunohistochemistry, all with advantages and disadvantages (Lane et al., 2022). Histology can be used in pathogen studies to help characterise the route of colonisation of organisms as it may allow for the evaluation of the presence, distribution and impact of an organism at defined time points in the host (Wang et al., 2021). The use of qPCR allows for discrimination of congeneric pathogens (Piesz et al., 2022, Ríos-Castro et al., 2022), and is useful to monitor the progress of an infection (Mackay et al., 2002). By monitoring pathogen infections in a host over an extended period, researchers can better understand the pathogenesis of the bacterial infection and develop effective strategies for mitigating its impact (Burge et al., 2016; DeCandia et al., 2018). For example, in the larvae of *M. edulis*, various *Vibrio* spp. and *Photobacterium* spp. isolates caused mortality after three days of infection, and genomic analyses identified virulence-related genes in the bacterial isolates responsible for the highest mortalities (Eggermont et al., 2017). In *P. canaliculus*, the effect of co-infection (using *P. swingsii* and *Vibrio mediterranei*) displayed varying responses overtime, with 100% mortality observed in juvenile mussels after 48 h, while adults showed the same results after 72 h (Azizan et al., 2023). The effect of sampling time was clearly seen in a study on *M. galloprovincialis* challenged with *V. splendidus*. Herein, two peaks of bacterial colonies were detected at 1 h and 6 h post challenge, demonstrating the recruitment of haemocytes and implementation of phagocytosis overtime (Parisi et al., 2019). Ultimately, strategies implemented by bacterial pathogens to avoid host defence mechanisms vary amongst species and can be complicated by different phases of infection (i.e., host-pathogen interactions or host immune response) (Labreuche et al., 2006).

The aim of this study was to evaluate the association between *P. swingsii* and adverse effects on the mussel, *P. canaliculus* overtime. *Photobacterium swingsii* DNA load and distribution in digestive gland, adductor muscle and gill tissues were evaluated over a 48-hour period post-challenge using qPCR and histopathology assessments. The mussel immune response was evaluated by haemolymph response (i.e., total haemocyte count and haemocyte viability) over the same period. We envision that these data will aid further studies into the pathological significance of *P. swingsii* and potential disease control alternatives.

2. Materials and methods

2.1. Animal husbandry, bacterial exposure, and sampling

Adult *P. canaliculus* (n = 300) were obtained from Kaiaua Marine Farms Ltd. (Firth of Thames, New Zealand) and transported to the aquaculture facility at the Auckland University of Technology, Auckland, New Zealand. Upon arrival, animals were labelled, weighed (mean ± SE, 53.8 ± 7.9 g) and measured along their length (90.5 ± 5.5 mm), and then housed for a 7-day acclimation period in a recirculating seawater system (16 °C; 35 ppt; pH 8.2).

Photobacterium swingsii was isolated from *P. canaliculus* during a 2018 mortality event (Nguyen and Alfaro, 2020), and grown to a pure culture on thiosulfate-citrate-bile salts sucrose (TCBS) agar plates, then cultured in marine broth (Difco™) and incubated at 22 °C for 24 h, as previously described by Azizan et al. (2022). For the present study, the bacterium was harvested, washed, and suspended in marine broth (Difco™) medium at a concentration of 10^7 colony forming units (CFU)/mL for injection treatments. To control for the effects of the handling and the act of injection, a second group of *P. swingsii* served as a heat-killed control group, where the inoculum of 10^7 CFU/mL was boiled at 100 °C for 10 min, before storage at 4 °C for 6 days. Inactivation of the bacteria was confirmed by culturing broth on TCBS agar plates for 6 days at 22 °C (Ciacci et al., 2009). No growth was observed over that period. Additional experimental groups included a group of untreated mussels (no injection control) and a group of mussels injected with marine broth (injection control).

A total of 75 mussels were allocated to each group (Fig. 1). At the onset of the experiment (time 0), 100 μL of either marine broth (G2), heat-killed *P. swingsii* suspended in marine broth (G3), or live *P. swingsii* suspended in marine broth (G4) (10^7 CFU/mL) were injected into the posterior adductor muscle of each individual mussel using a 25-gauge 1 mL syringe. In order to facilitate the injection, mussels were gently opened on the ventral posterior side of the shell using a blunt knife (Ericson et al., 2022). The presence of the injected bacterial isolate in the haemolymph samples was confirmed using the Sanger sequencing method (see Table S1). After injection, all mussels including the no injection controls (G1) were placed into individual 2-L tanks with seawater and air supply. Mussel survival was monitored for 4 days, using the British Standard Squeeze method which classified a mussel as dead if the animal was unable to adduct valves following 10 rapid squeezes (Dunphy et al., 2015; Powell et al., 2017; Nguyen et al., 2020). Dead mussels were removed from the system and sexed accordingly. Daily water exchanges (50% of total volume) were performed along with water quality assessment of four parameters, namely, pH, ammonia, nitrite, and nitrate using a Marine Saltwater Master Test Kit (API Marine) (Azizan et al., 2022). The survival rate was calculated as the survival probability at any particular time (S*t*) (Goel et al., 2010), determined by the equation:

$$St = (Numberofsubjectslivingatthestart - Numberofsubjectsthatdied) \times 100$$

After 12 hpc (time 1), 24 hpc (time 2) and 48 hpc (time 3), a total of 10 mussels per group were sampled (apart from the no-injection control which was only tissue sampled at the end – 48 h). Mussels were opened to collect a haemolymph sample from the adductor muscle (Ericson et al., 2023). For bacterial plating, a 10 μL aliquot of haemolymph was spread onto a TCBS agar plate using the spread plate technique (Demann and Wegner, 2019). All plates were incubated at 22 °C for 24–48 h before being counted to obtain CFU/mL of Vibrionaceae load in the haemolymph (Azizan et al., 2022). Following haemolymph collection, 5 individual mussels were used for histological sample collection, while a second set of 5 mussels were used for tissue collection for qPCR testing.

For flow cytometric analyses, a working haemolymph stock was first prepared with 50 μL of haemolymph diluted equally with the same volume of autoclaved filtered seawater. A total of 20 μL of the working haemolymph stock was added to 380 μL of Muse® Count & Viability Kit (200X, MCH100104; Luminex). The sample was vortexed, incubated at 18 °C for 5 min before analysis using a Muse Cell Analyzer (Ericson et al., 2021).

For histological assessments, mussels (n = 50) were shucked and placed in 10 % formalin in seawater for 48 h, whereafter the animals were cut into 2 histology sections, the first containing the adductor muscle (point of injection) tissue and the second section containing all the major organs (gill, mantle, digestive gland, gonad, connective tissue, and foot). Once cut and placed in histology cassettes, standard histological processing followed (Muznebin et al., 2022). The mussels were examined by a veterinary pathologist and examined blind with no knowledge of the study groups. Body condition scoring was scored as follows: 1+ indicated poor condition, 2+ denoted moderate to good condition, and 3+ signified excellent condition. Scoring for all organ systems evaluated was a subjective, semi-quantitative assessment. In judging body condition consideration was given to the degree of expansion of storage cells, width of storage cell trabeculae and the

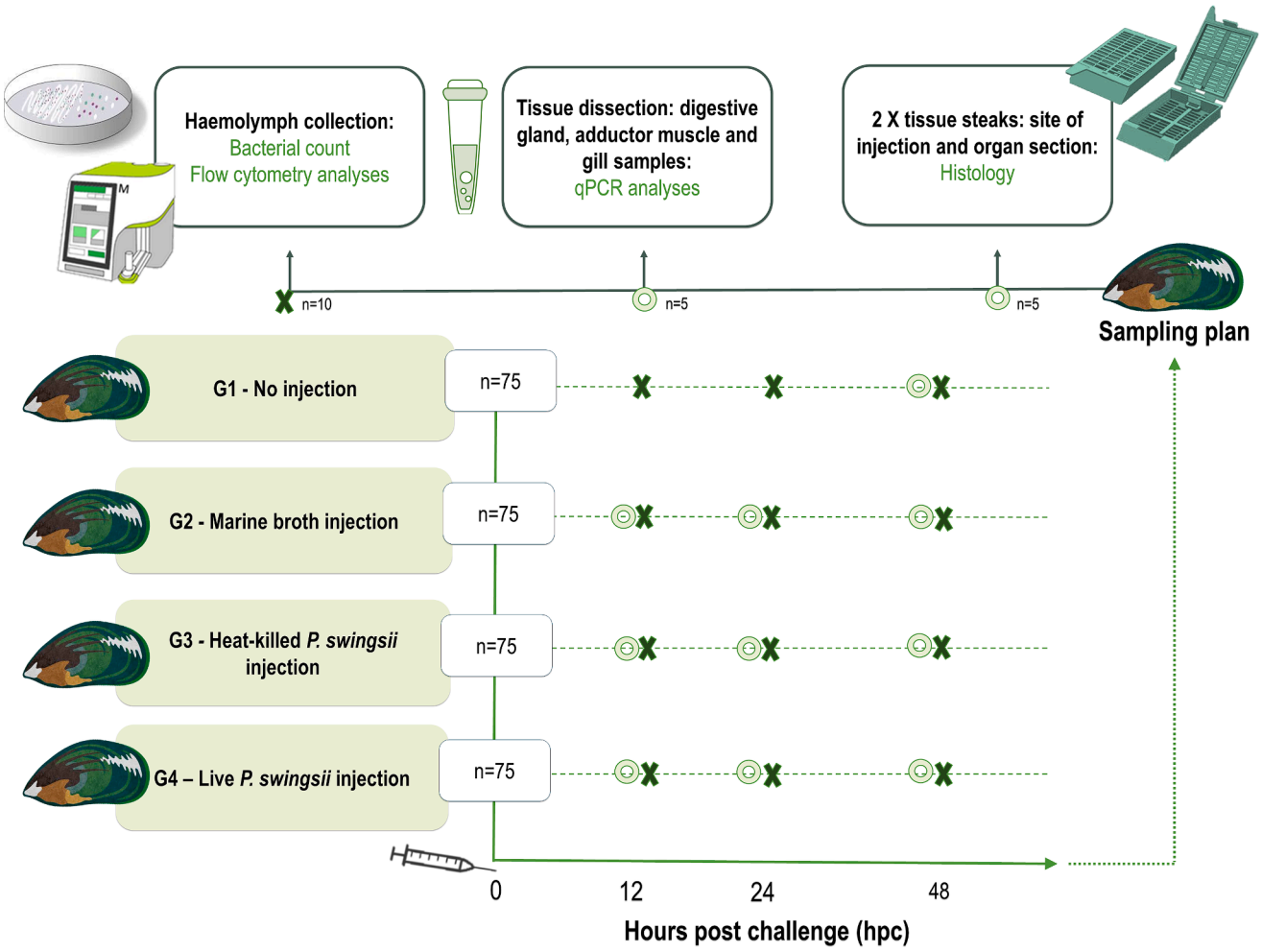

Fig. 1. Experimental setup: *Perna canaliculus* mussels were assigned four groups, including G1 = no injection control, G2 = control injected with marine broth, G3 = control injected with heat-killed bacteria, and G4 = treatment injected with live bacteria. Mussels were sampled after 12-, 24- and 48-hours post-challenge. At each sampling point, haemolymph was collected for flow cytometry and bacterial quantification and tissue samples for qPCR and sections for histological assessments (note, tissue samples for no injection control group were only collected at 48 hpc). Abbreviations: X = a total of 10 mussels per group were sampled, except for the no injection control, which was only tissue sampled at the end (48 hpc); O = a total of 5 individual mussels were used for histological sample collection, while a second set of 5 mussels were used for tissue collection for qPCR testing.

presence, absence, and width of intercellular and vascular spaces between storage cell trabeculae and connective tissues. The digestive glands were evaluated for tubular uniformity, cell composition and structure of the tubular and ductular epithelium, presence or absence of epithelial degeneration or changes, presence of inflammatory cells within the epithelium and lumen of tubules and ducts, presence, absence, density, extent, and pattern of haemocyte infiltrates within supporting connective tissue around digestive gland tubules and ducts and surrounding the intestinal tract.

For qPCR testing, mussels from each treatment were shucked and the digestive gland, adductor muscle and gill tissues were removed. Tissue samples of about 3 × 3 mm in size were placed into separate microcentrifuge tubes containing 200 µL RNAlater® and refrigerated for an hour to permeate the solution into tissue before storage in a −80 °C freezer until DNA extraction was performed.

2.2. TaqMan qPCR for Photobacterium swingsii

2.2.1. DNA extraction

Tissues (adductor muscle, gill, digestive gland) from 50 mussels were extracted using the simple workflow of the MagMAX™ Core Nucleic Acid Purification Kit (Applied Biosystems™) executed on an automated KingFisher™ Flex system. Prior to extraction, tissues were removed from RNAlater, washed in phosphate buffered saline (PBS) and then homogenised in the same, using 1.4 mm diameter ceramic beads in a MagNA Lyser (Roche Diagnostics, Basel, Switzerland), 6500 rpm, 30 s. The weight data was collected to enable comparative measurements of copy numbers across individuals. Tissue input weights ranged from 23.4 to 32.4 mg, with an average of 26 mg. Each sample corresponded to 2 µL of DNA template obtained from a specified tissue input amount. No-injection control, marine broth injection control and bacteria-infected mussel (killed *P. swingsii* and live *P. swingsii*) samples were then tested with a PCR specific for the *P. swingsii* 16S rRNA gene.

2.2.2. qPCR design and procedure

Primers and hybridising probe were designed using the Geneious Prime software (Dotmatics) to target the *P. swingsii* 16S rRNA genes. Geneious Prime and Primer BLAST were used to assess *in-silico* the specificity of the assay. PCR mix comprised of 12.5 µL SsoAdvanced™ Universal Probes Supermix (Bio-Rad), 8 µL nuclease free water, 1 µL (400 nM) of each primer, *P. swingsii* – 229F-5′GGTCCATTTTCTGGCATGGC3′ and *P. swingsii* – 324R-5′TTGTGGCGACGATACACCAA3′; 0.5 µL of the probe (200 nM), *P. swingsii*-282P FAM-AGTTGACGGCGTACTCCTTG-BHQ1; and 2 µL of DNA template. The reaction was run on a CFX96 (Bio-Rad) thermocycler with the following conditions: 1 cycle of 95 °C for 3 min, followed by 40 cycles of 95 °C for 30 s and 60 °C for 30 s (Caraguel

et al., 2011). Results were analysed using CFX Manager™ software.

Each qPCR included a set of standards prepared using *P. swingsii* genomic DNA (dilutions from known CFU concentrations) and no-template controls. A PCR run was considered valid when the standards were detected, and the no-template controls were not detected. All samples from valid runs showing a *Cq* before the 40 cycles cut-off were considered positive. Quantification of *P. swingsii* in samples was calculated by the software based on the standard curve.

2.3. Statistical analysis

A two-way ANOVA was performed to assess the combined effects of time and treatment on experimental data (including bacterial load, total haemocyte counts, cell viability, and qPCR). Subsequently, Bonferroni post-hoc tests were then used to compare experimental groups at specific timepoints, considering the significant influence of time. PCR quantitative data was log-transformed to deal with the wide range of results due to natural variations in the data. For the log transformation, the lowest copy number result for any sample was added to all results to remove the impossibility of transformation for values = 0. All data met assumptions for normality (Shapiro-Wilk Test, $p > 0.05$) and for homogeneity of variances (Levene's test, $p > 0.05$). A p-value < 0.05 was considered statistically significant. Statistical analyses were performed in GraphPad Prism® version 9 (San Diego, CA).

3. Results

3.1. Mussel survival

During the 72-hour monitoring period, mussel survival remained 100% for the no-injection control group (G1), the marine broth injection group (G2), and the heat-killed bacterial injection group (G3). Within the group injected with live *P. swingsii* (G4), mortalities started to occur 24 h post-challenge (hpc), with a 63.5% survival rate seen at the end of three days. Statistically, G4 differed from the other experimental groups (log-rank test, $p < 0.001$; Fig. 2, as denoted by lowercase letters).

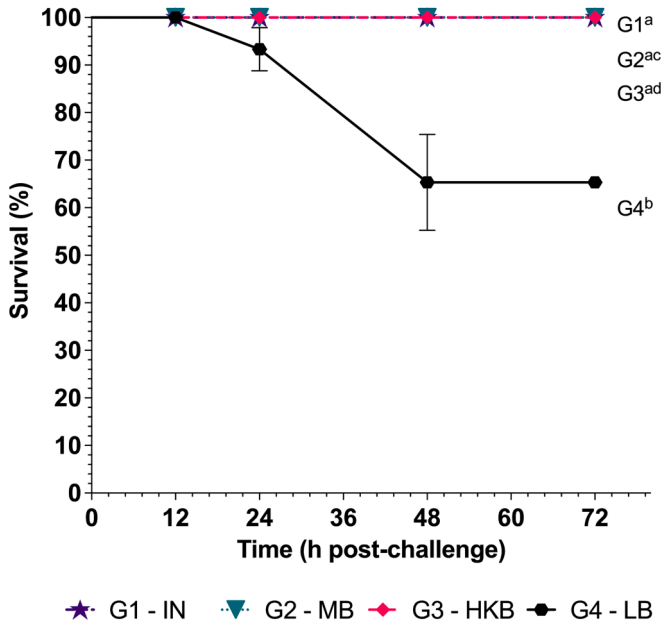

Fig. 2. Survival curves for *Perna canaliculus* mussel following no injection (G1 – IN *), injection with marine broth (G2 – MB ▼), injection with heat-killed bacteria (G3 – HKB ◆), and injection with live *P. swingsii* bacteria (G4 – LB ⬣). Significant differences of log-rank (Mantel-Cox) test are indicated by different lowercase letters next to each survival curve when comparing the live bacteria injection group to the other groups ($p < 0.001$).

3.2. Bacterial quantification

The number of bacterial colony forming units (CFU) counted with characteristics of Vibrionaceae, within samples of mussel haemolymph within treatments (G1-G4) at 12, 24 and 48 hpc, are reported in Fig. 3. Amongst treatment groups, at all sampling timepoints, haemolymph from mussels injected with live *P. swingsii* (G4) showed the largest number of CFU. Within G4, after 12 hpc, 43 CFU were detected. At 24 hpc, this value was two-fold higher with 109 CFU detected, and at 48 hpc the largest number of bacterial counts, of 273 CFU were detected. These changes were statistically significant when comparing the bacterial concentrations within G4 between timepoints 12 hpc and 48 hpc ($p < 0.001$) and between 24 hpc and 48 hpc ($p < 0.001$). Moreover, there was an interaction effect among treatment groups and sampling timepoint (Timepoint*Treatment, $p < 0.001$, 2-way ANOVA).

3.3. Haemocyte count and haemocyte viability

The total number of haemocytes (THC) and haemocyte viability (% live haemocytes) detected in mussel haemolymph after 12, 24 and 48 hpc are shown in Fig. 4a and 4b, respectively. Within the first three control groups, samples at 12 hpc resulted in the greatest haemocyte counts when mussels were not treated (G1 = mean ± SE, $3.9 \times 10^6 \pm 5.7 \times 10^5$ cells/mL), injected with marine broth (G2 = $3.6 \times 10^6 \pm 8.7 \times 10^5$ cells/mL), and injected with heat-killed bacteria ($3 \times 10^6 \pm 5.9 \times 10^5$ cells/mL). A decrease in haemocyte counts was determined as time progressed with 48 hpc showing the lowest number of haemocytes.

Contrastingly, the group injected with live *P. swingsii* (G4) displayed a noticeable trend over time, with numerical fluctuations. While it is notable that the lowest number of haemocytes were detected at 12 hpc, and the highest number of haemocytes detected at 48 hpc (Fig. 4a), multiple comparisons (Bonferroni's test) revealed no statistically significant differences within the group injected with *P. swingsii* (G4). Two-way ANOVA revealed no significance related to treatment ($p = 0.3126$), whereas sampling timepoint had a statistically significant effect ($p = 0.0310$). There was a significant interaction between treatment groups and time ($p = 0.0343$, 2-way ANOVA) as seen in the no injection control group at 48 hpc.

For haemocyte viability, similar levels of haemocytes were measured at 12 hpc within all treatments (G1: 72 ± 3.3%; G2: 75 ± 2.8%; G3: 66 ± 3.7%; G4: 66 ± 4.1%). All treatments (G1-G4) showed similar patterns as time progressed with an increase in haemocyte viability seen at 24 hpc followed by a decrease at 48 hpc (Fig. 4b). The 2-way ANOVA revealed a non-statistically significant effect of the treatment group ($p = 0.3529$) and the sampling timepoint ($p = 0.2144$) for the percentages of cell viability. The effect of treatment did not differ between timepoints (Timepoint*Treatment, $p = 0.942$).

3.4. qPCR

Following qPCR analyses, positive amplification signals were obtained from adductor muscle tissue (Fig. 5a) at 24 hpc in mussels injected with heat-killed *P. swingsii* (G3), and at 12, 24 and 48 hpc in mussels injected with live *P. swingsii* (G4). In the gill tissue (Fig. 5b), positive amplification signals were seen at 24 hpc in mussels injected with marine broth, at 24, and 48 hpc in G3, and at 12, 24 and 48 hpc in G4. The digestive gland tissue (Fig. 5c) showed positive amplification signals at 24 hpc in G3 and at 12, 24 and 48 hpc in G4. The bacterial DNA in mussel tissues injected with heat-killed bacteria (G3) was on average 5.81 gene copies per mussel (across tissues collected = 76.25 copies per mg of tissue) for all samples collected through the experiment. In mussels injected with live *P. swingsii* (G4), the average bacterial load was 29-fold greater – 163.2 copies per sample (2,141 copies per mg of tissue).

This difference in bacterial DNA between G3 and G4 was highly significant across all sampling times (12, 24 and 48 h) for all tissues

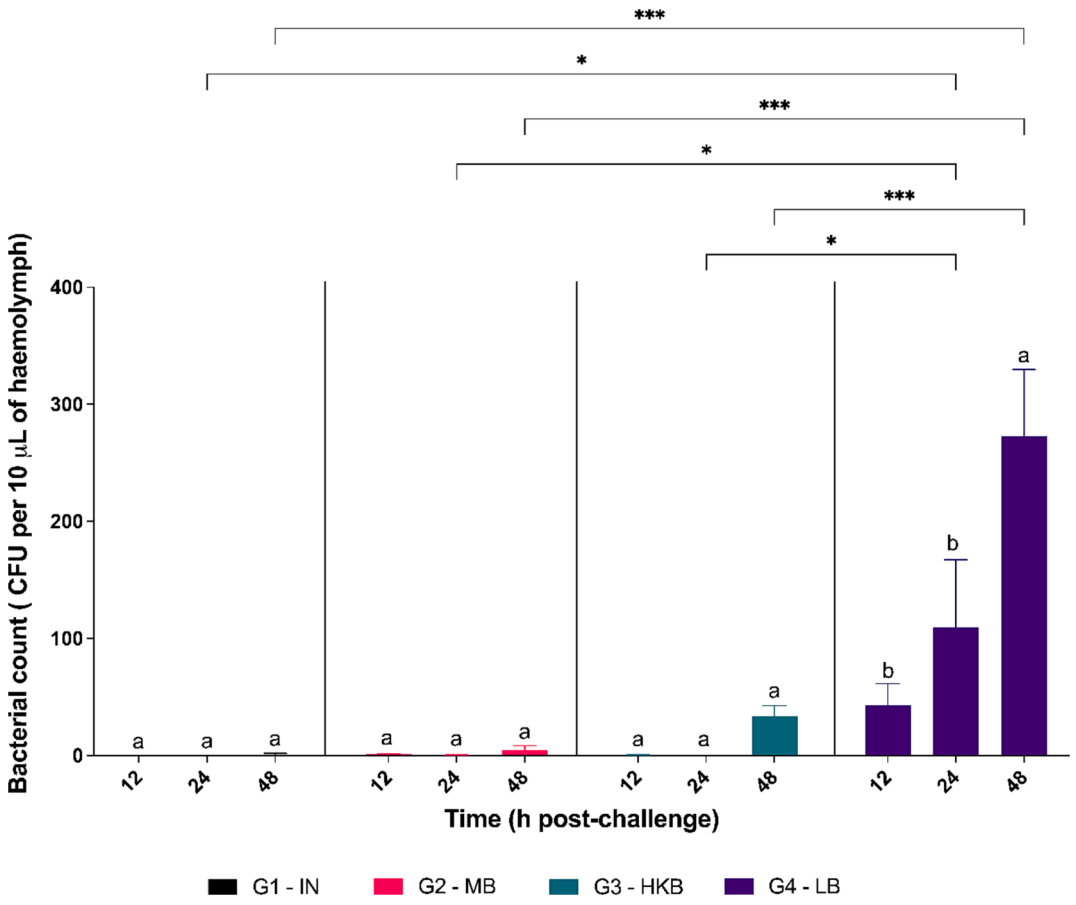

Fig. 3. Quantification of Vibrionaceae colony forming units (CFU per 10 µL of haemolymph) obtained from haemolymph of the G1 – no injection (control), G2 – marine broth (injection control), G3 heat-killed and G4 live bacteria challenged groups at 12, 24, 48-hpc. All values represent average of 10 replicates per treatment. Error bars represent standard error of means (SEM). The hatching bracket between 2 bars represent significant differences between groups at the same timepoint. The single asterisk (*) represents a significant difference at $p < 0.05$, double asterisks (**) are for a difference at $p < 0.001$ and triple asterisks (***) are for a difference at $p < 0.0001$. The different letters (e.g., a and b) indicate comparisons between timepoints within the same groups.

analysed (2-way ANOVAs; $p < 0.001$, respectively). Across treatments, time did not have a significant effect on bacterial load and there was no significant interaction between time and treatment (2-way ANOVA; $p > 0.05$). Similarly, the bacterial load was not significantly different for the tissue types evaluated, adductor muscle, gill, and digestive gland (2-way ANOVA; p-value > 0.05).

3.5. Histopathology

Histopathological assessments were performed on all *P. canaliculus* mussels sampled over time (12, 24 and 48 hpc) and across treatment groups (G1–G4), as summarised in Table 1. In brief, the histopathological assessments focused on the body condition, distribution, and intensity of inflammation in the tissues, gonad development, digestive gland, connective tissues, gills, and mantle.

Variable infiltrates of inflammatory cells and haemocytes were present within the connective tissues of all mussels examined during the study, as seen within the control group (Fig. 6a), the marine broth injected control group (Fig. 6c), the heat-killed bacterial injection group (Fig. 6e), and the live bacterial injection group (Fig. 6j). The digestive glands in all mussels examined had non-specific changes consisting of variable digestive gland atrophy and early degenerative changes affecting the basophilic cells of the digestive glands with occasional inflammation affecting the glands directly (Fig. 6b, d, f). The gill tissues across treatments presented normal with occasional low levels of haemocyte infiltrates (Fig. 6k). The adductor muscle of mussels subjected to experimental injection (G2, 3 and 4) showed evidence of tissue degeneration and haemocyte infiltration presumed to be associated with the site of injection (Fig. 6h). The mantle showed variable inflammation with scattered nodular to diffuse haemocyte infiltrates (Fig. 6g, j) across all treatments. One mussel sampled (1/5) (G4T1) from the live *P. swingsii* injection group at 48 hpc had a focal area of marked inflammation within the connective tissue associated with short rod-shaped bacteria (Fig. 6h), and one mussel (G4T2) had an incidental finding of birefringent organism resembling microsporidian like organism (Fig. 6l). Occasional bacteria were recognised within areas of muscle necrosis associated with the injection site of the live *P. swingsii* (Fig. 6h). Mussels within G4 also showed moderate to good body condition and female gonadal tissue (Fig. 6i) and normal gills (Fig. 6k).

4. Discussion

Herein we discuss for the first-time results based on bacterial progression of a *P. swingsii* challenge in Greenshell™ mussels, *P. canaliculus*. Our study revealed that injection with *P. swingsii* induced host response and mortalities while mussels injected with heat-killed *P. swingsii* and marine broth survived. This further supports the hypothesis that *P. swingsii* is pathogenic to mussels and despite the limitations posed by the challenge of mussels using injection of the adductor muscle, we found that live bacteria induced pathogenesis, while heat-killed bacteria did not. This indicates that the mortalities are due to bacterial proliferation rather than the injury caused by the injection itself.

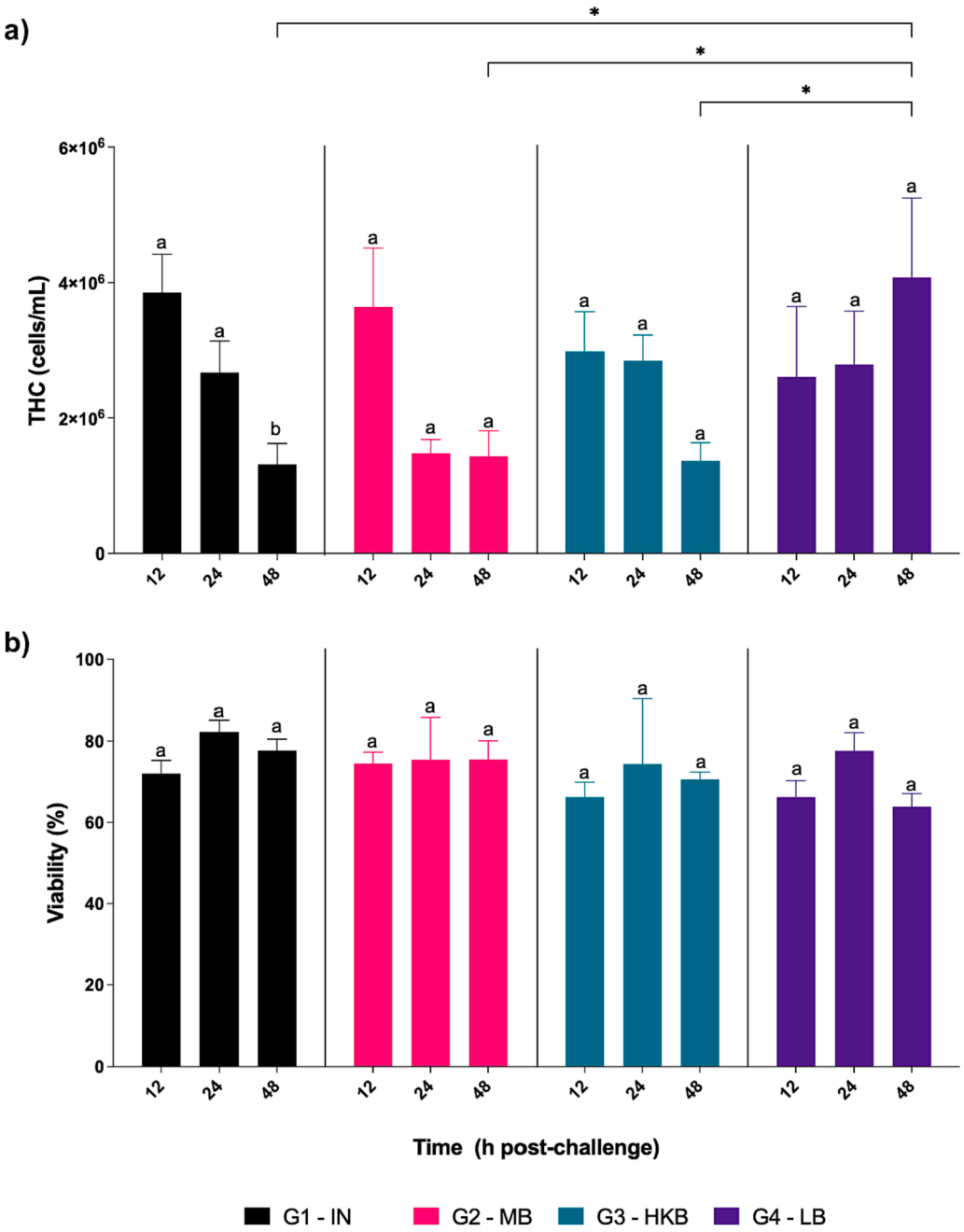

Fig. 4. (a) Total haemocyte counts, and (b) haemocyte viability changes of *Perma canaliculus* mussels in the G1 - no injection (control), G2 - marine broth (injection control), G3 heat-killed and G4 live bacteria challenged groups at 12, 24, 48-hpc. The hatching bracket between 2 bars represent significant differences between groups at the same timepoint. The single asterisk (*) represents a significant difference at $p < 0.05$, double asterisks (**) are for a difference at $p < 0.001$ and triple asterisks (***) are for a difference at $p < 0.0001$. The different letters (e.g., a and b) indicate comparisons between timepoints within the same groups. All values represent average of 10 replicates per treatment. Error bars represent standard error of means (SEM).

4.1. Mussel response

No mortalities were observed in the control groups investigated in the current study, as previously seen in control treatments utilising *P. canaliculus* as an animal model (Azizan et al., 2022). Haemocyte viability was measured to quantify the amount of live or dead cells in a haemocyte population of mussels (Tresnakova et al., 2023), and our results found no major changes in haemocyte viability status recorded amongst control groups or timepoints. Similarly, insignificant changes were detected in haemocyte viability profiles in *P. canaliculus* subjected to temperature and pathogen stress, along with the corresponding controls (Azizan et al., unpublished results).

Total haemocyte counts (THC) in molluscs are generally an indicator of organism health and immune status (Ericson et al., 2023), with increasing circulating haemocytes associated with the presence of a stressor (Venter et al., 2021). At the first sampling point, (12 hpc), the number of haemocytes in the three control groups were the highest, potentially because of experimental holding (husbandry stress), while the lowest THC were detected at 48 hpc. Interestingly, the opposite THC response was seen in the group of mussels infected with live *P. swingsii*, where the lowest number of haemocytes were detected at 12 hpc, and the highest at 48 hpc. A previous study on Greenshell™ mussels reported a decrease in haemocyte concentration in the *Vibrio* spp. treated group (compared to controls) after 24 h of infection (Ericson et al., 2022). Then

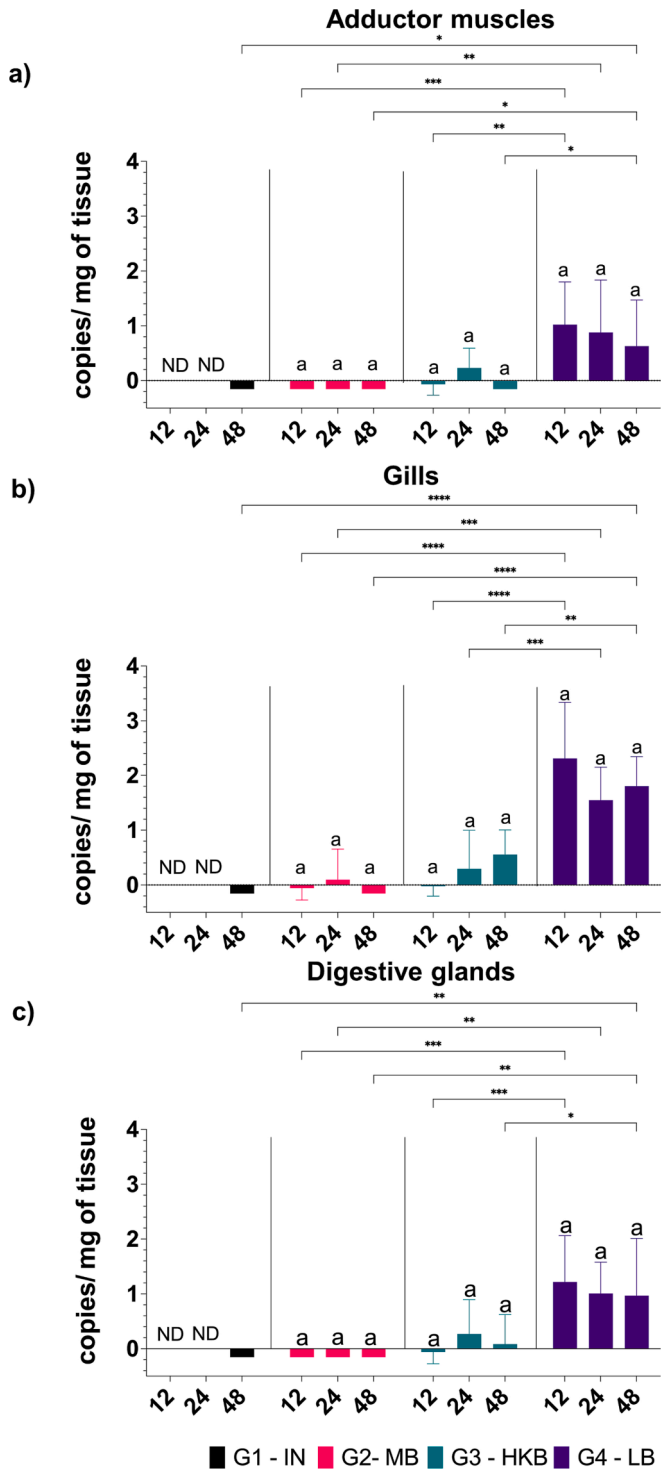

Fig. 5. Bar graphs of log-transformed bacterial loads, which represents the concentration + 0.70 copies/sample (0 values replaced with minimum dataset value, followed by data transformation to log scale as measured by qPCR analyses from (a) adductor muscle, (b) gill and (c) digestive gland tissue samples across treatments (G1 – no injection control, only sampled at 48 h; G2 - marine broth injection; G3 - heat-killed bacterial injection, and G4 - live bacteria injection) at 12, 24, 48-hpc. Each sample corresponds to 2 μL of DNA template obtained from a specified tissue input amount.

again, when injecting clams, *Ruditapes philippinarum,* with live bacteria a loss of haemocytes was seen in the early phase of infection (Parisi et al., 2019). A loss of haemocytes at the onset of infection are believed to be due to the clearance of high initial bacterial loads, migration of haemocytes from the haemocoel to the injection site, lysis of haemocytes, or apoptosis of haemocytes after phagocytosis of bacteria (Mateo et al., 2009, Parisi et al., 2019). However, in the current study, as time progressed, the THC increased after exposure to bacterial infection, suggesting that the haemocytes multiplied as a systemic response to stress (i.e., *P. swingsii* injection).

Colony forming units (CFU) were counted as a key predictor of bacterial presence (Quinn et al., 2022). Greenshell™ mussels injected with a live dose of *P. swingsii* displayed the highest CFU (compared to the other three groups), with CFU also increasing with time, resulting in the highest concentrations of bacterial colonies at 48 hpc. Thus, by two days post-challenge, bacteria within the haemolymph of *P. canaliculus* had not been cleared from the mussels' circulation system. It has been previously reported that *V. splendidus* bacteria were present in the haemolymph of *M. galloprovincialis* for 24 hpc, while *V. anguillarum* was still present in the haemolymph of the same species at 48 hpc (Parisi et al., 2008). Ultimately, the kinetics of bacterial clearance remains variable based on the bacteria and bivalve species (Canesi et al., 2001). It should also be kept in mind that CFU were only measured in the mussels that survived the infection process, making the results a measure of mussels that are in the process of fighting the *P. swingsii* injection.

Mussel survival is a primary determinant of relative fitness (Shields et al., 2008). It is used as an end-point measure in the current study to determine the effect of *P. swingsii* on mussel physiology. The higher mortality observed in mussels injected with live *P. swingsii* potentially occurred due to the inability of mussels to clear bacteria from the haemolymph. In contrast, heat-killed bacteria did not cause any mussel mortalities in the current study. This outcome of zero mortality has been previously reported in *Ruditapes philippinarum* injected with heat-killed *V. tapetis*, while the mortality of clams injected with live bacteria was attributed to the actions of the bacteria rather than influence of extracellular virulence factors (Allam et al., 2002).

4.2. Quantifying *P. swingsii*

For the first time, bacterial quantification from *P. swingsii*-specific PCR is reported in this study. Herein, mussels injected with live and heat-killed *P. swingsii* showed detectable levels of bacteria, albeit higher in the group receiving the live dose of *P. swingsii.* Variations of *P. swingsii* DNA loads were detected within the adductor muscle, gill and digestive gland tissues investigated at all timepoints, indicating that *P. swingsii* spread into the internal organs potentially resulting in systemic infection. The quantification of *P. swingsii* DNA loads before 12 hpc remains an interesting aspect for future studies. In the current study we did not observe any clear trend of reduced or increased quantified bacteria overtime, as only three time points were studied, making it impossible to declare links to bacterial clearance as time continues. It is believed that a longer exposure duration, larger sample sizes, or shorter sampling timepoints would allow for a more precise quantification of bacterial loads which can be used to establish changes in bacterial load overtime. Amongst the tissues analysed in the present study, the bacterial DNA detected in the gill tissue was the greatest, which might hint at its important role in the immune response during pathogen challenge (Li et al., 2017). Indeed, the quantification of *P. swingsii* DNA loads in tissue samples will aid future research on this topic considering mussel tissues role in antimicrobial mechanisms (Bachère et al., 2015).

4.3. *P. swingsii* within mussel tissues

Histological findings from this study showed aggregation of haemocytes along with haemocyte infiltration, in the cross-section of the whole animal, suggestive of inflammatory cells migrating to a point in

Table 1
Summary of the histopathological assessments of Greenshell™ mussel tissues from four treatment groups (no injection control, only sampled at 48 h; marine broth injection; heat-killed *Photobacterium swingsii* injection and live *P. swingsii* injection) across sampling timepoints per 5 mussels observed (x/5).

Time post challenge	12 h			24 h			48 h			
Treatment	G2	G3	G4	G2	G3	G4	G1	G2	G3	G4
Haemocytes infiltrations within tissue types										
Gills	2/5 NAD 3/5 (1 + S)	5/5 (1 + S)	5/5 (1 + S)	5/5 (1 + S)	5/5 (1 + S)	5/5 (1 + S)	4/5 NAD 1/5 (1 + S)	5/5 (1 + S)	3/5 (1 + S) 2/5 (NAD)	5/5 NAD
Mantle	2/5 NAD 1/5 (1 + S) 1/5 (1 + F) 1/5 (1 + N)	1/5 (1 + S) 2/5 (1/2 + D) 1/5(1 + M) 1/5(1/2+)	2/5(1 + S) 2/5 (1 + M) 1/5(1 + F)	3/5 (1 + S) 2/5 (1/2 + M)	2/5 (1/2 + M) 1/5(1 + M) 1/5 (2+) 1/5 (2/3 + M)	2/5 (1 + M) 1/5(1/2 + NAD)2/5 (1 + S)	2/5(1 + S/N) 1/5(1 + S/D) 1/5 (2 + D) 1/5 (2/3 + NAD)	3/5 (NAD) 1/5 (1/2 + S) 1/5 (1/2 + M)	3/5 (1 + S) 2/5 (NAD	2/5 (1 + S) 3/5 (NAD
Digestive gland	5/5 (NR)	4/5 (HI) 1/5 (NR)	3/5 (HI) 2/5 (NR)	5/5 (NR)	2/5 (HI) 3/5 (NR)	1/5 (2 + HA) 1/5 (2 + HI) 3/5 (NR)	3/5 (HI) 1/5 (PR) 1/5(NR)	4/5 (HI) 1/5 (NR)	2/5 (HI) 3/5 (NR)	1/5 (HI) 4/5 (NR)
Dilation of digestive gland										
Mild (1+)	4/5	1/5	3/5	0	2/5	0	3/5	4/5	4/5	4/5
Mild to moderate (1/2+)	0	4/5	1/5	1	2/5	4/5	1/5	1/5	0	0
Moderate (2+)	0	0	0	0	1/5	1/5	1/5	0	0	0
Moderate to heavy (2/3+)	1/5	0	0	0	0	0	0	0	0	0
Heavy (3+)	0	0	1/5	0	0	0	0	0	0	0
Not represented	0	0	0	0	0	0	0	1/5	1/5	1/5
Body condition score										
Poor (1+)	0	0	0	0	1/5	1/5	0	0	0	0
Poor to moderate (1/2+)	1/5	4/5	0	1/5	1/5	1/5	0	0	1/5	0
Moderate (2+)	0	0	0	2/5	2/5	2/5	2/5	2/5	1/5	1/5
Moderate to excellent (2/3+)	0	0	3/5	2/5	0	1/5	3/5	1/5	1/5	4/5
Excellent (3+)	4/5	1/5	2/5	0	1/5	0	0	2/5	2/5	0
Inflammation based on connective tissues of mantle and gill (1st area) & digestive gland tubules (2nd area)										
Mild (1+)	0	0	4/5	3/5	3/5	0	2/5	4/5	1	4/5
Mild to moderate (1/2+)	2/5	2/5	0	2/5	0	4/5	0	1/5	0	0
Moderate (2+)	3/5	2/5	1/5	0	2/5	0	2/5	0	0	0
Moderate to heavy (2/3+)	0	1/5	0	0	0	1/5	1/5	0	0	0
Heavy (3+)	0	0	0	0	0	0	0	0	0	1/5
Adductor muscle degeneration and necrosis with haemocyte infiltrates										
Minimal	1/5 (MD + HI)	0	3/5 (MDN + HI)	4/5 (MDN + HI)	3/5 (MDN + HI)	1/5 (MDN + HI)	0	0	0	0
Mild (1+)	2/5 (MD + HI)	0	1/5 (MDN + HI)	0	1/5 (MDN + HI)	4/5 (MDN + HI)	1/5 (MD)	0	1/5 (MD + HI)	0
Mild to moderate (1/2+)	0	0	0	0	0	0	0	0	0	0
Moderate (2+)	0	0	1/5 (MDN + HI)	0	0	0	1/5 (MD)	0	1/5 (MD + HI)	2/5 (MD + HI)
Moderate to heavy (2/3+)	0	0		0	0	0	0	0	0	0
Heavy (3+)	1/5 (MD + HI)	0		0	0	0	0	0	0	0
Not represented	1/5	5/5		1/5	1/5	0	0	5/5	3/5	3/5
Presence or absence of bacteria										
Absence	5/5	5/5	3/5	1	4/5	1	0	1	4/5	4/5
Presence	0	0	2/5	0	1/5	0	0	0	1/5	1/5
Questionable	0	0	0	0	0	0	0	0	0	0
Apicomplexan-like/Microsporadia like/Haplosporidian/microcell like organisms	2/5	1/5	2/5	0	0	3/5	1/5	0	0	0

Abbreviations: G1 = No injection, G2 = Marine broth injection, G3 = Heat-killed bacteria injection, G4 = Live bacteria injection; NAD = Nodular and diffuse; S = Scattered; F = Focal; N = Nodular; D = Diffuse; M = Multifocal; P = Poorly represented; NR = Not represented; HI = Haemocyte infiltration; HA = Haemocyte aggregation; MD = muscle degeneration; MDN = muscle degeneration and necrosis.

response to a stimulus. This observation of inflammation is not specific to a cause, but could indicate an unspecified adaptation response of mussels to laboratory conditions (Cajaraville et al., 1991), inadequate nutrition (Sokolova et al., 2012), natural physiological processes, such as spawning (Wendling and Wegner, 2013) or breakdown products (Van de Braak et al., 2002). Inflammation can also be a consequence of bacterial infection (Buckley et al., 2017, Jarc and Petan, 2019, Pudgerd et al., 2021), as seen in *P. viridis* exposed to *V. alginolyticus* (Laith et al., 2021), yet the effects of *P. swingsii* are difficult to discern from the current data, perhaps reflecting the short duration of the exposure or injection dose administrated. Incidental histological findings included detection of birefringent organism within the male gonad germinal cells and focally in the connective tissue of one mussel. These findings are likely associated with the fact that mussels were sourced from a

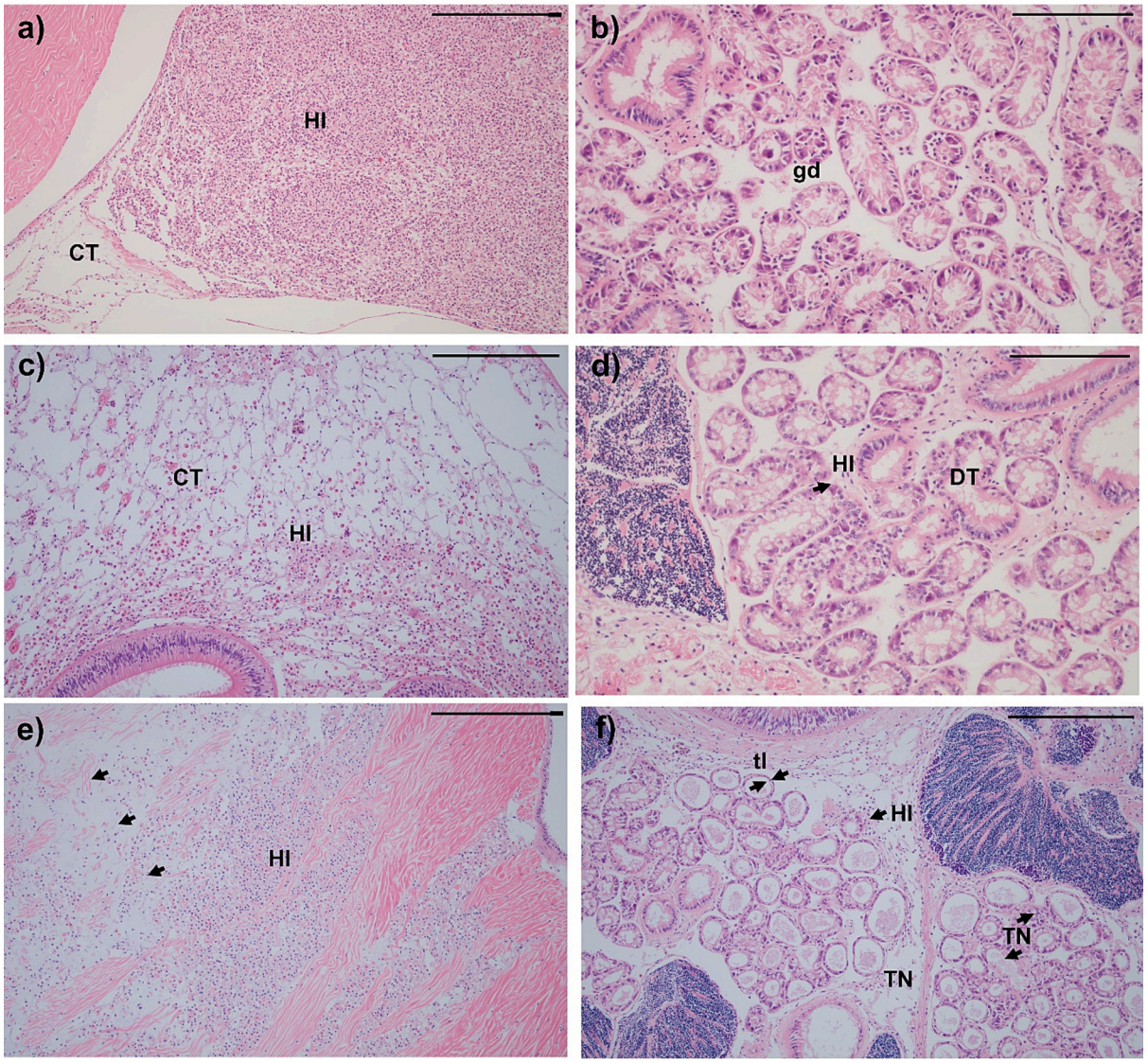

Fig. 6. Histopathological alterations observed in *Perna canaliculus* following (a, b) no injection (G1); (c, d) injection with marine broth (G2) and (e, f) injection with heat killed bacteria (G3). (a) Marked haemocyte infiltration (HI) with nodular distribution in the connective tissues (CT) (20×). (b) Digestive gland disruption (gd) rounding of basophil cells and digestive epithelial cells detaching from basement membrane, without significant signs of inflammation (20×). (c) Haemocyte infiltration (HI) with mild to moderate inflammation of the connective tissue (CT). (d) Mild digestive tubule (DT) dilation with focal mild inflammation (HI) affecting the tubule epithelium and lumen (40×). (e) Mantel with dense haemocyte infiltration (HI) and oedema of the connective tissue. (f) Marked dilation of digestive tubules (tl, white arrow); with epithelial change and degeneration in various tubules. Mild stromal haemocyte infiltration (HI, black arrow) in the digestive gland (20×). Fig. 6 cont. Histopathological alterations observed in *Perna canaliculus* injected with live bacteria (G4). (g) Necrotic tissue (TN) with haemocyte (hm) aggregation, and fluid accumulation within the adductor muscle (20×). (h) Tissue degeneration (white arrows), haemocyte (hm) aggregation around the infection site. Inset; bacteria free in connective tissue (40×). (i) Example of mussel with moderate to good body condition and female gonadal tissue (4×). (j) Haemocyte infiltration (HI) and mild inflammation of the connective tissue (CT) (20×). (k) Normal gills (20×). (l) Birefringent organism (BO), viewed with polarising filter (polarisers) (40×). Scale bar used for figures a, c, e, f, g, j, k = 200 μM; for figures b, d, h, I = 100 μM and figure i = 500 μM.

commercial open seawater aquaculture facility and not a pathogen-free colony/culture. They do not appear to have adversely affected the findings of this study.

In this study, inflammation in the gills was minimal within all experimental groups with no significant differences between them. The occurrence of gill inflammation, has been reported in clams with no link to damage to gill epithelia, but rather as a consequence of environmental variables (e.g., waterborne particles) (Costa et al., 2013). Resultantly, small changes in gill structure are to be expected, as seen in the current study, as gills are delegate structures, directly affected by external stimuli. Changes within the digestive glands, associated with dilation of the digestive lumen, atrophy of the gland epithelium and dissociation of the cells were detected across treatments and timepoints. Within bivalves the disruption of some digestive cells are considered a normal physiological process of digestion (Usheva et al., 2006). Also the housing of mussels in an aquarium setup has previously shown disintegration of digestive cells within the epithelium due to manipulation and aerial exposure (Dimitriadis and Koukouzika, 2003). Thus, the morphological changes expressed by the digestive gland from all the mussels in the current study can be attributed to the disintegration phase of digestion and/or the effect of holding in the laboratory.

The adductor muscle tissues around the site of injection across treatments were characterised by muscle degeneration and necrosis with haemocytic infiltration. Such changes can be due to trauma from the

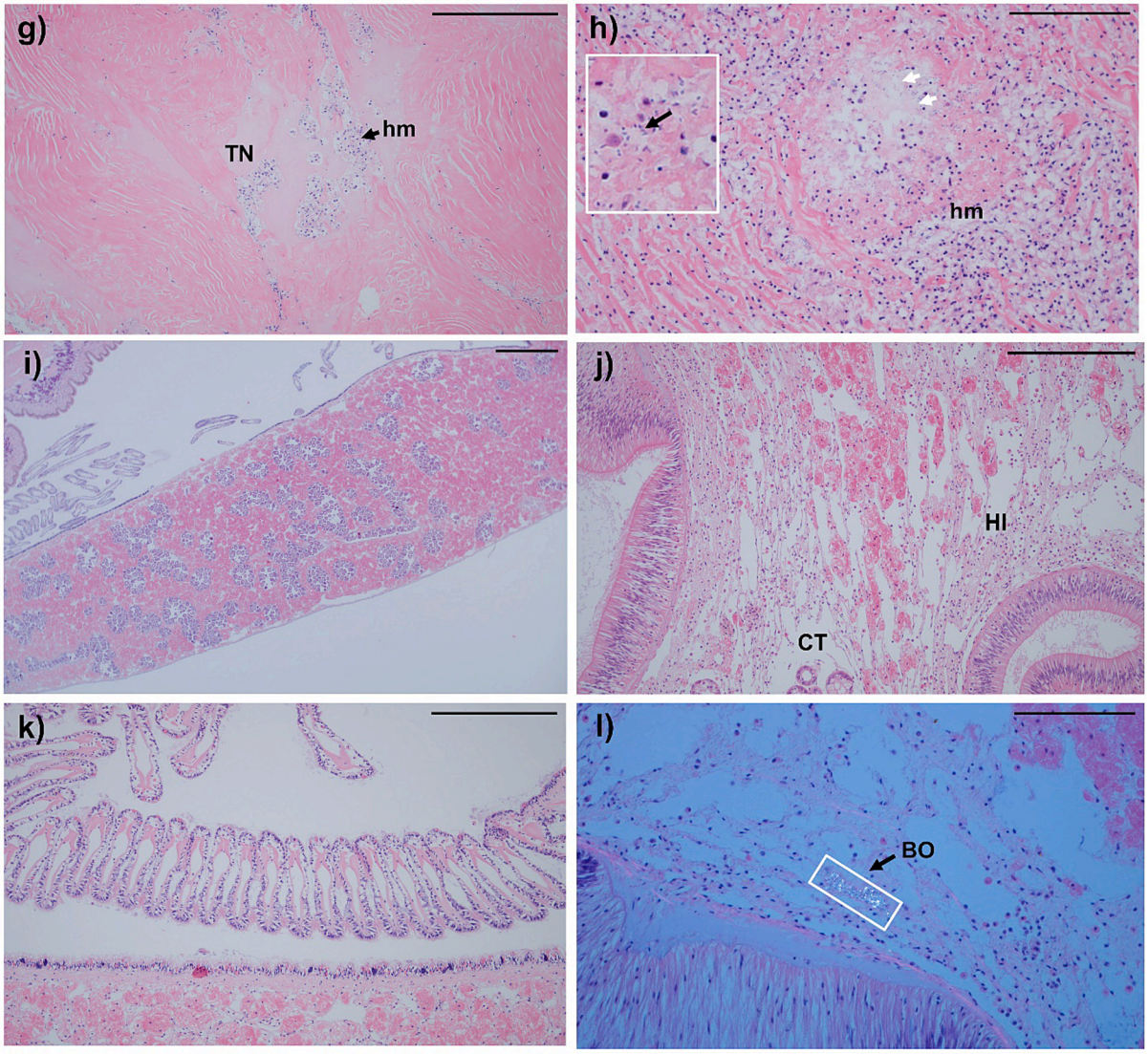

Fig. 6. (*continued*).

injection where the possible hydrostatic pressure of injecting material/fluid, results in sterile tissue degradation (Wang, 2018). The same lesions were evident in all treatments without any specific link to *P. swingsii* injection. Bacterial injections into adductor muscle are known to cause local inflammation at the injection site (Allam et al., 2002). Previous studies on *Macrobrachium rosenbergii*, *Litopenaeus vannamei* and *Crassostrea gigas* reported necrosis of the muscle cells infiltrated with accumulating haemocytes following infections with *Vibrio* (*V. alginolyticus* and *V. splendidus*) (Gay et al., 2004, Liu and Chen, 2004, Ajadi et al., 2019). Injuries to tissue are seen as a breach of the first defence barrier (Gay et al., 2004), resulting in a general stress response as seen in the adductor muscle samples of the injected mussels under investigation. In *M. galloprovincialis* a recruitment of haemocytes along with changes in the volume of muscular fibres were reported at the bacterial site of injection. Yet, recovery of the muscle tissue organisation followed by 48 h of injection (Parisi et al., 2019). In *P. canaliculus* the effect of injection was still evident following 48 h, requiring more research to define the tissue recovery period.

In conclusion, this evaluation of *P. swingsii* pathogenesis in *Perna canaliculus* shows physiological changes due to bacterial injection overtime. At 48 hpc, mussels injected with *P. swingsii* showed the highest mortality rates, haemocytes counts and bacterial colony forming units. The bacterial quantification supported systemic infection of mussel tissues with *P. swingsii* overtime. The histopathological results showed injury obtained due to injection of treatments to the adductor muscle, along with the activation of an unspecific inflammatory response or the activation of defence mechanisms via cell proliferation. No clear link was established between the qPCR results (*P. swingsii* DNA load) and the presence of inflammatory cells.

To gain a better understanding on the susceptibility of mussels toward *P. swingsii* infection, further studies will require an assessment of the entire immune system including humoral factors, since cellular factors alone do not provide a complete picture of infection outcomes. The species-specific qPCR developed in this study can potentially be used for wider surveillance programmes to study the epidemiology of *P. swingsii* on mussel farms. Ultimately, this study supports efforts to strengthen biosecurity management and aquatic surveillance workstreams.

Funding

This project was funded by the New Zealand Ministry of Business, Innovation and Employment (MBIE; 'Aquaculture health strategies to maximise productivity and security', contract no. CAWX1707) under a collaborative program between AUT and the Cawthron Institute (Nelson, New Zealand), with additional support from the Animal Health

Laboratory, Ministry for Primary Industries.

CRediT authorship contribution statement

Awanis Azizan: Conceptualization, Data curation, Formal analysis, Investigation, Methodology, Writing – original draft, Writing – review & editing. **Andrea C. Alfaro:** Conceptualization, Funding acquisition, Resources, Supervision, Writing – review & editing. **Leonie Venter:** Conceptualization, Data curation, Formal analysis, Investigation, Methodology, Project administration, Resources, Supervision, Writing – original draft, Writing – review & editing. **Diana Jaramillo:** Formal analysis, Investigation, Methodology, Resources, Supervision, Writing – review & editing. **Mark Bestbier:** Investigation, Resources, Writing – review & editing. **Peter Bennett:** Investigation, Methodology, Resources, Writing – review & editing. **Jonathan Foxwell:** Data curation, Formal analysis, Methodology, Resources, Writing – review & editing. **Tim Young:** Formal analysis, Investigation, Methodology, Writing – review & editing.

Declaration of competing interest

The authors declare that they have no known competing financial interests or personal relationships that could have appeared to influence the work reported in this paper.

Acknowledgments

Thank you to Kaiaua Mussel Farms for providing the mussels for experimental purposes. Thanks to technicians at the School of Science at Auckland University of Technology and members of the Aquaculture Biotechnology Research Group for their assistance and support during all stages of this study. A big thanks goes out to Shaneel Sharma and Ronald Lulijwa for their hands-on assistance in the wet lab. Thank you to the scientists at the Bacteriology and Aquatic Animal Diseases laboratory, Ministry for Primary Industries for guidance, support, and input with this project.

Appendix A. Supplementary material

https://doi.org/10.1016/j.jip.2024.108065

References

Ajadi, A., Sabri, M., Atata, J., Daodu, O., Emikpe, B., 2019. Pathology and immunohistochemical evaluation of *Vibrio alginolyticus* infection in *Macrobrachium rosenbergii*. Comp. Clin. Pathol. 28, 359–368.

Allam, B., Paillard, C., Ford, S.E., 2002. Pathogenicity of *Vibrio tapetis*, the etiological agent of brown ring disease in clams. Dis. Aquat. Organ. 48, 221–231.

Azizan, A., Alfaro, A.C., Jaramillo, D., Venter, L., Young, T., Frost, E., Lee, K., van Nguyen, T., Kitundu, E., Archer, S.D.J., Ericson, J.A., Foxwell, J., Quinn, O., Ragg, N. L.C., 2022. Pathogenicity and virulence of bacterial strains associated with summer mortality in marine mussels (*Perna canaliculus*). FEMS Microbiol. Ecol. 98, 1–14.

Azizan, A., Carter, J., Alfaro, A.C., Venter, L., Young, T., Sharma, S.S., Chen, T., 2023. Investigating the effect of bacterial co-infections on juvenile and adult, green-lipped mussels (*Perna canaliculus*). J. World Aquac. Soc. 1–18.

Bachère, E., Rosa, R.D., Schmitt, P., Poirier, A.C., Merou, N., Charrière, G.M., Destoumieux-Garzon, D., 2015. The new insights into the oyster antimicrobial defense: cellular, molecular and genetic view. Fish Shellfish Immunol. 46, 50–64.

Buckley, K.M., Ho, E.C.H., Hibino, T., Schrankel, C.S., Schuh, N.W., Wang, G., Rast, J.P., 2017. IL17 factors are early regulators in the gut epithelium during inflammatory response to *Vibrio* in the sea urchin larva. Elife 6, e23481.

Burge, C.A., Closek, C.J., Friedman, C.S., Groner, M.L., Jenkins, C.M., Shore-Maggio, A., Welsh, J.E., 2016. The use of filter-feeders to manage disease in a changing world. Integr. Comp. Biol. 56, 573–587.

Cajaraville, M., Díez, G., Marigómez, I., Angulo, E., 1991. Consequences of keeping *Mytilus* in the laboratory as assessed by different cellular condition indices. Helgoländer Meeresuntersuchungen 45, 445–464.

Canesi, L., Pruzzo, C., Tarsi, R., Gallo, G., 2001. Surface interactions between *Escherichia coli* and hemocytes of the Mediterranean mussel *Mytilus galloprovincialis* Lam. leading to efficient bacterial clearance. Appl. Environ. Microbiol. 67, 464–468.

Caraguel, C.G., Stryhn, H., Gagné, N., Dohoo, I.R., Hammell, K.L., 2011. Selection of a cutoff value for real-time polymerase chain reaction results to fit a diagnostic purpose: analytical and epidemiologic approaches. J. Vet. Diagn. Invest. 23, 2–15.

Castinel, A., Webb, S., Jones, J., Peeler, E., Forrest, B., 2019. Disease threats to farmed green-lipped mussels *Perna canaliculus* in New Zealand: review of challenges in risk assessment and pathway analysis. Aquac. Environ. Interact. 11, 291–304.

Ciacci, C., Citterio, B., Betti, M., Canonico, B., Roch, P., Canesi, L., 2009. Functional differential immune responses of *Mytilus galloprovincialis* to bacterial challenge. Compar. Biochem. Physiol.-B Biochem. Mol. Biol. 153, 365–371.

Costa, P.M., Carreira, S., Costa, M.H., Caeiro, S., 2013. Development of histopathological indices in a commercial marine bivalve (*Ruditapes decussatus*) to determine environmental quality. Aquat. Toxicol. 126, 442–454.

Decandia, A.L., Dobson, A.P., Vonholdt, B.M., 2018. Toward an integrative molecular approach to wildlife disease. Conserv. Biol. 32, 798–807.

Demann, F., Wegner, K.M., 2019. Infection by invasive parasites increases susceptibility of native hosts to secondary infection via modulation of cellular immunity. J. Anim. Ecol. 88, 427–438.

Dimitriadis, V.K., Koukouzika, N., 2003. Effect of sampling procedures, transportation stress and laboratory maintenance on the structure and function of the digestive gland epithelium of the mussel *Mytilus galloprovincialis*. Mar. Biol. 142 (5), 915–924.

Dunphy, B.J., Watts, E., Ragg, N.L.C., 2015. Identifying thermally-stressed adult green-lipped mussels (*Perna canaliculus* Gmelin, 1791) via metabolomic profiling. Am. Malacol. Bull. 33, 127–135.

Eggermont, M., Bossier, P., Pande, G.S.J., Delahaut, V., Rayhan, A.M., Gupta, N., Islam, S.S., Yumo, E., Nevejan, N., Sorgeloos, P., Gomez-Gil, B., Defoirdt, T., 2017. Isolation of *Vibrionaceae* from wild blue mussel (*Mytilus edulis*) adults and their impact on blue mussel larviculture. FEMS Microbiol. Ecol. 93, 1–11.

Ericson, J.A., Ragg, N.L.C., Rolton, A., 2021. Flow cytometric validation of a commercial kit to assess the concentration and viability of bivalve hemocytes. Fish Shellfish Immunol. 119, 452–455.

Ericson, J.A., Venter, L., Welford, M.R.V., Kumanan, K., Alfaro, A.C., Ragg, N.L.C., 2022. Effects of seawater temperature and acute *Vibrio* sp. challenge on the haemolymph immune and metabolic responses of adult mussels (*Perna canaliculus*). Fish Shellfish Immunol. 128, 664–675.

Ericson, J.A., Venter, L., Copedo, J.S., Nguyen, V.T., Alfaro, A.C., Ragg, N.L.C., 2023. Chronic heat stress as a predisposing factor in summer mortality of mussels, *Perna canaliculus*. Aquaculture 564, 738986.

Fichi, G., Cardeti, G., Perrucci, S., Vanni, A., Cersini, A., Lenzi, C., de Wolf, T., Fronte, B., Guarducci, M., Susini, F., 2015. Skin lesion-associated pathogens from *Octopus vulgaris*: first detection of *Photobacterium swingsii*, *Lactococcus garvieae* and betanodavirus. Dis. Aquat. Organ. 115, 147–156.

Gay, M., Renault, T., Pons, A.M., le Roux, F., 2004. Two *Vibrio splendidus* related strains collaborate to kill *Crassostrea gigas:* taxonomy and host alterations. Disease of Aquatic Organism 62, 65–74.

Goel, M.K., Khanna, P., Kishore, J., 2010. Understanding survival analysis: Kaplan-Meier estimate. Int. J. Ayurveda Res. 1, 274.

Gomez-Gil, B., Roque, A., Rotllant, G., Peinado, L., Romalde, J.L., Doce, A., Cabanillas-Beltrán, H., Chimetto, L.A., Thompson, F.L., 2011. *Photobacterium swingsii* sp. nov., isolated from marine organisms. Int. J. Syst. Evol. Microbiol. 61, 315–319.

Jarc, E., Petan, T., 2019. Focus: Organelles: Lipid droplets and the management of cellular stress. Yale J. Biol. Med. 92, 435.

Jiang, Q., Shi, L., Ke, C., You, W., Zhao, J., 2013. Identification and characterization of *Vibrio harveyi* associated with diseased abalone *Haliotis diversicolor*. Dis. Aquat. Organ. 103, 133–139.

Kesarcodi-Watson, A., Kaspar, H., Lategan, M., Gibson, L., 2009. Two pathogens of Greenshell™ mussel larvae, *Perna canaliculus*: *Vibrio splendidus* and a *V. coralliilyticus*/neptunius-like isolate. J. Fish Dis. 32, 499–507.

Labella, A.M., Arahal, D.R., Castro, D., Lemos, M.L., Borrego, J.J., 2017. Revisiting the genus Photobacterium: taxonomy, ecology and pathogenesis. Int. Microbiol. 20, 1–10.

Labreuche, Y., Lambert, C., Soudant, P., Boulo, V., Huvet, A., Nicolas, J.-L., 2006. Cellular and molecular hemocyte responses of the Pacific oyster, *Crassostrea gigas,* following bacterial infection with *Vibrio aestuarianus* strain 01/32. Microbes Infect. 8 (12-13), 2715–2724.

Laith, A.A., Ros-Amira, M.K., Sheikh, H.I., Effendy, A.W.M., Najiah, M., 2021. Histopathological and immunological changes in green mussel, *Perna viridis*, challenged with *Vibrio alginolyticus*. Fish Shellfish Immunol. 118, 169–179.

Lane, H.S., Brosnahan, C.L., Poulin, R., 2022. Aquatic disease in New Zealand: synthesis and future directions. N. Z. J. Mar. Freshw. Res. 56, 1–42.

Li, Y., Song, X., Wang, W., Wang, L., Yi, Q., Jiang, S., Jia, Z., Du, X., Qiu, L., Song, L., 2017. The hematopoiesis in gill and its role in the immune response of Pacific oyster *Crassostrea gigas* against secondary challenge with *Vibrio splendidus*. Dev. Comp. Immunol. 71, 59–69.

Liu, C.H., Chen, J.C., 2004. Effect of ammonia on the immune response of white shrimp *Litopenaeus vannamei* and its susceptibility to *Vibrio alginolyticus*. Fish Shellfish Immunol. 16, 321–334.

Mackay, I.M., Arden, K.E., Nitsche, A., 2002. Real-time PCR in virology. Nucleic Acids Res. 30, 1292–1305.

Mateo, D.R., Siah, A., Araya, M.T., Berthe, F.C.J., Johnson, G.R., Greenwood, S.J., 2009. Differential in vivo response of soft-shell clam hemocytes against two strains of *Vibrio splendidus*: changes in cell structure, numbers and adherence. J. Invertebr. Pathol. 102, 50–56.

Miller, M.R., Abshirini, M., Wolber, F.M., Tuterangiwhiu, T.R., Kruger, M.C., 2023. Greenshell mussel products: a comprehensive review of sustainability, traditional use, and efficacy. Sustainability 15, 3912.

Muznebin, F., Alfaro, A.C., Webb, S.C., 2022. *Perkinsus olseni* and other parasites and abnormal tissue structures in New Zealand Greenshell™ mussels (*Perna canaliculus*) across different seasons. Aquac. Int. 1–36.

Nguyen, T.V., Alfaro, A.C., 2020. Metabolomics investigation of summer mortality in New Zealand Greenshell™ mussels (*Perna canaliculus*). Fish Shellfish Immunol. 106, 783–791.

Nguyen, T.V., Ragg, N.L.C., Alfaro, A.C., Zamora, L.N., 2020. Physiological stress associated with mechanical harvesting and transport of cultured mussels (*Perna canaliculus*): a metabolomics approach. Aquaculture 529, 735657.

Parisi, M.-G., Li, H., Jouvet, L.B., Dyrynda, E.A., Parrinello, N., Cammarata, M., Roch, P., 2008. Differential involvement of mussel hemocyte sub-populations in the clearance of bacteria. Fish Shellfish Immunol. 25, 834–840.

Parisi, M.G., Maisano, M., Cappello, T., Oliva, S., Mauceri, A., Toubiana, M., Cammarata, M., 2019. Responses of marine mussel *Mytilus galloprovincialis* (Bivalvia: Mytilidae) after infection with the pathogen *Vibrio splendidus*. Comp. Biochem. Physiol. C: Toxicol. Pharmacol. 221, 1–9.

Piesz, J.L., Scro, A.K., Corbett, R., Lundgren, K.M., Smolowitz, R., Gomez-Chiarri, M., 2022. Development of a multiplex qPCR for the quantification of three protozoan parasites of the eastern oyster *Crassostrea virginica*. Dis. Aquat. Organ. 151, 111–121.

Powell, J., Ragg, N., Dunphy, B., 2017. Phenotypic biomarkers in selectively-bred families of the Greenshell™ mussel (*Perna canaliculus*): Anaerobic enzyme and shell gape behaviour as biomarkers of prolonged emersion tolerance. Aquaculture 479, 601–608.

Pudgerd, A., Kruangkum, T., Sritunyalucksana, K., Vanichviriyakit, R., Imsonpang, S., Chotwiwatthanakun, C., 2021. Immunopathogenesis of hematopoietic tissues in response to *Vibrio parahaemolyticus* (VPAHPND) infection in *Macrobrachium rosenbergii*. Fish Shellfish Immunol. 110, 10–22.

Quinn, E.A., Malkin, S.H., Thomas, J.E., Poole, R., Davies, C.E., Rowley, A.F., Coates, C. J., 2022. Invasive slipper limpets (*Crepidula fornicata*) act like a sink, rather than source, of *Vibrio* spp. Biol. Invasions 24, 3647–3659.

Ríos-Castro, R., Aranguren, R., Romero, A., Banchi, E., Pallavicini, A., Novoa, B., Figueras, A., 2022. Assessment of the environmental distribution of the protozoan parasite *Perkinsus olseni* by next-generation sequencing, qPCR and histopathology allows the identification of alternative bivalve hosts. Aquaculture 552, 737984.

Shields, J.L., Barnes, P., Heath, D.D., 2008. Growth and survival differences among native, introduced and hybrid blue mussels (*Mytilus* spp.): genotype, environment and interaction effects. Mar. Biol. 154 (5), 919–928.

Sokolova, I.M., Frederich, M., Bagwe, R., Lannig, G., Sukhotin, A.A., 2012. Energy homeostasis as an integrative tool for assessing limits of environmental stress tolerance in aquatic invertebrates. Mar. Environ. Res. 79, 1–15.

Tresnakova, N., Famulari, S., Zicarelli, G., Impellitteri, F., Pagano, M., Presti, G., Filice, M., Caferro, A., Gulotta, E., Salvatore, G., Sandova, M., Vazzana, I., Imbrogno, S., Capillo, G., Savoca, S., Velisek, J., Faggio, C., 2023. Multi-characteristic toxicity of enantioselective chiral fungicide tebuconazole to a model organism Mediterranean mussel *Mytilus galloprovincialis* Lamarck, 1819 (Bivalve: Mytilidae). Sci. Total Environ. 862, 160874.

Usheva, L., Vaschenko, M., Durkina, V., 2006. Histopathology of the digestive gland of the bivalve mollusk *Crenomytilus grayanus* (Dunker, 1853) from southwestern Peter the Great Bay, Sea of Japan. Russ. J. Mar. Biol. 32, 166–172.

van de Braak, C., Botterblom, M., Taverne, N.V., van Muiswinkel, W., Rombout, J., van der Knaap, W., 2002. The roles of haemocytes and the lymphoid organ in the clearance of injected *Vibrio* bacteria in *Penaeus monodon* shrimp. Fish Shellfish Immunol. 13, 293–309.

Venter, L., Young, T., Alfaro, A.C., Lindeque, J.Z., 2021. Establishing sampling confidence parameters: Effect OF sampling and transport conditions on haemocyte and metabolite profiles of Greenshell mussels. Aquaculture 538, 736538.

Wang, J., 2018. Neutrophils in tissue injury and repair. Cell Tissue Res. 371, 531–539.

Wang, D., Loor, A., Bels, L.D., Stappen, G.V., Broeck, W.V.D., Nevejan, N., 2021. Dynamic immune response to vibriosis in Pacific oyster *Crassostrea gigas* larvae during the infection process as supported by accurate positioning of GFP-tagged Vibrio strains. Microorganisms 9, 1523.

Webb, S., Duncan, J., 2019. New Zealand shellfish health monitoring 2007 to 2017: insights and projections. Cawthron Report No. 2568. Cawthron Report.

Wendling, C.C., Wegner, K.M., 2013. Relative contribution of reproductive investment, thermal stress and *Vibrio* infection to summer mortality phenomena in Pacific oysters. Aquaculture 412, 88–96.